Diagn Interv Radiol 2021; 27:710–715

CHEST IMAGING

ORIGINAL ARTICLE

Role of magnetic resonance spectroscopy in differential diagnosis of solitary pulmonary lesions

Azad Hekimoglu
Onur Ergun
Aynur Turan
Tugba Taskin Turkmenoglu
Baki Hekimoglu

PURPOSE
The aim of our study was to evaluate the availability of magnetic resonance spectroscopy (MRS) for the differentiation of benign or malignant pulmonary nodules and masses.

METHODS
A total of 59 patients (45 male, 14 female) with pulmonary nodules and masses were included in this prospective study. MRS was applied to the pulmonary lesions of the patients and choline levels were determined. Afterwards CT-guided percutaneous needle biopsy was performed. According to the biopsy results, pulmonary lesions were benign in 25 patients and malignant in 34 patients.

RESULTS
Choline levels were significantly higher in malignant lesions compared with benign lesions ($p < 0.001$). When the other conditions were kept constant, the probability of malignancy significantly increased by 17.38-fold (95% CI, 3.78–79.93) in those with choline levels >1.65 µmol/g compared to those with choline levels ≤1.65 µmol/g ($p < 0.001$).

CONCLUSION
MRS is a noninvasive method that can be used in the differential diagnosis of pulmonary nodules and masses.

The majority of the solitary pulmonary nodules have a benign character (1). However, all pulmonary nodules should be considered as malignant lesions unless proven otherwise (2). The differential diagnosis of these lesions may be an important problem in routine medical practice. Computed tomography (CT) is the standard method for the examination of the nodules and mass lesions (3). CT imaging of morphological features like size, margins, and calcification enables the investigation of malignancy (4). However, there is some overlap so that some malignant lesions may appear benign, while some benign nodules may show morphological features typical for malignancy (5). CT imaging for differantial diagnosis have problems like false-negative and false-positive results, over-diagnosis, benign nodule resections, and exposure to radiation (6). Biopsy is the most reliable and effective method for the diagnosis of the pulmonary nodules and mass lesions. However, it may cause serious complications such as pneumothorax, hemoptysis, air embolism, tumor cell seeding and death (7, 8). In addition, the tolerability of this invasive intervention is rather low among patients.

Magnetic resonance imaging (MRI) provides information about the tumor morphology and magnetic resonance spectroscopy (MRS) provides biochemical information about the physiology and metabolism of the disease (9). MRS enables molecular analysis of the tissues based on the display of different chemical shifts of certain nuclei in the magnetic field (10). MRS was initially used in neuroradiology for characterization of tumor, stroke, epilepsy, infection, and neurodegenerative diseases. In recent years, it was also introduced in the evaluation of lesions in other organs like breast (11), liver (12), pancreas (13), and prostate (14). There are some *in vitro* studies in the literature on the use of MRS in lung cancer showing higher lactate and total choline peaks compared with normal tissues (15, 16). Also there is one case report in the literature regarding the feasibility of using MRS in lung cancer (17).

Department of Radiology (A.H. ✉ *azadhekimoglu@gmail.com*), Diskapi Yildirim Beyazit Training and Research Hospital, Ankara, Turkey.

Received 4 June 2020; revision requested 26 June 2020; last revision received 8 September 2020; accepted 19 October 2020.

Published online 21 September 2021.

DOI 10.5152/dir.2021.20419

You may cite this article as: Hekimoglu A, Ergun O, Turan A, Taskin Turkmenoglu T, Hekimoglu B. Role of magnetic resonance spectroscopy in differential diagnosis of solitary pulmonary lesions. Diagn Interv Radiol 2021; 27:710–715

The objective of this study was to demonstrate the value of MRS, which is a noninvasive method and does not require a contrast agent, in the differential diagnosis of pulmonary nodules and mass lesions.

Methods

A total of 59 adult patients (45 males, 14 females) with pulmonary nodule or mass lesion, were included in the study. All of these patients were undiagnosed and therefore planned for percutaneous lung biopsy. Inclusion criteria for our study were: patients over 18 years old and able to provide written informed consent, intrapulmonary tumors larger than 1 cm in diameter on CT images, and patients accepting percutaneous lung biopsy. Our exclusion criteria were patients in whom MRI was contraindicated, intractable cough, inability to lie flat or other impediment to acquisition of breath-hold MRI, and patients for whom percutaneous lung biopsy is unsuitable for technical reasons.

On CT images, 6 of the benign lesions had irregular margins, 2 of them had calcifications, 3 of them had lobulated contours, 2 of them had spiculations and 3 of them had cavitation, whereas 21 of the malignant lesions had irregular margins, 7 of them had lobulated contours, 2 of them had spiculations and 2 of them had cavitation. However, there was no significant morphological feature in the rest of the benign and malignant nodules.

The size of the largest and smallest lesions were 50 mm and 14 mm, respectively (Table 1). The median (25^{th}–75^{th}) percentile of the maximum lesion size for all cases was 35 mm (23–50 mm) and the median (25^{th}–75^{th}) percentile of the minimum lesion size was 26 mm (17–38 mm).

First, single-voxel proton MRS was performed to the pulmonary lesions. Thereafter, a percutaneous biopsy was performed by the department of interventional radiology. A 22G Chiba needle was used for the biopsy. Percutaneous biopsies were carried out under the supervision of a cytopathologist and the intervention was repeated until adequate samples were obtained. According to the results of the pathological examination, 25 lesions were benign (18 males, 7 females; mean age, 61.3±15.9 years) and 34 lesions were malignant (27 males, 7 females; mean age, 67.3±9.3 years) (Table 1).

Table 1. Demographical and clinical characteristics

	Benign (n=25)	Malignant (n=34)	*p*
Age (years), mean±SD	61.3±15.9	67.3±9.3	0.070[a]
Gender, n (%)			0.72[b]
Male	18 (72.0)	27 (79.4)	
Female	7 (28.0)	7 (20.6)	
Lesion size (mm), median (min–max)			
Maximum	25 (18–47.5)	38 (27–50)	0.083[c]
Minimum	19 (14–32.5)	28.5 (21–40)	0.023[c]
Pack-years cigarette smoking, median (min–max)	0 (0–18.8)	30 (0–46.2)	0.042[c]
Localization, n (%)			0.78[b]
Right	15 (60.0)	18 (52.9)	
Left	10 (40.0)	16 (47.1)	
Localization, n (%)			0.23[d]
Upper	8 (32.0)	18 (52.9)	
Middle	3 (12.0)	4 (11.8)	
Lower	14 (56.0)	12 (35.3)	
Choline, median (min–max)	0.60 (0.02–3.22)	5.80 (2.21–11.30)	<0.001[c]

[a]Student t test; [b]Continuity corrected chi-square test, [c]Mann–Whitney U test, [d]Fisher–Freeman–Halton exact test.

Our study had a prospective design and was conducted according to the ethical standards of the Helsinki Declaration and was approved by the Institutional Ethics Committee (17/32).

MR spectroscopy technique

Spectroscopic evaluation was performed with 1.5 T MRI Scanner (Gyroscan Intera, Philips) and sense 8 channel body coil was used. In this study, breast MRS application was used. Single-voxel proton (^{1}H) spectroscopy and the point-resolved spatially localized spectroscopy (PRESS) (TR, 2000 ms; TE, 50 ms; flip angle, 90°; readout duration, 512 ms; spectral resolution, 1.95 Hz) was used for the MRS examination. The voxel volume was minimum 1 cm^3 depending on the size of the lesion.

Also, three-plan T2-weighted turbo spin-echo–cardiac triggering sequence (TR/TE, 2000/90 ms; acquisition voxel, 1.37×1.71×5 mm^3; matrix, 256×160; flip angle, 90°; slice thickness of 5 mm, slice gap 1 mm) was conducted for the placement of the spectroscopy voxel. The voxel was adjusted to cover a minimum of 80% of the lesion for a good spectrum and high signal/noise ratio. Care was taken that there was no lung air left in the voxel. In lesions with cystic and necrotic component, the voxel was placed on the solid part of the lesion (Fig. 1). After automated shimming, manual shimming adjustment was performed using linear shimming orders. In addition, because the lung is a mobile organ and patients could not hold their breath for a long time, the procedure was tried to be kept short.

The chemical shift scale has the 1–7 ppm range and the metabolites have sufficient concentration, they are expressed as micromoles per gram (μmol/g). On proton MRS, choline-containing metabolites peak at 3.2 ppm (parts per million), water at 4.7 ppm and lipids at 1.3 ppm (18). In our study, choline peak values obtained by supressing water and lipid were calculated (Fig. 2).

Cytopatological examination

For all cases on-site cytological evaluation was done by a cytopathologist. Cytological material was prepared using conventional method. Once the slides were determined as sufficient, remaining sample was collected into neutral buffered formalin for cell block preparation. Diff-Quik stain was used for rapid specimen adequacy assessment. Rest of the slides were stained with MGG.

Main points

- MRS can be used in the differential diagnosis of pulmonary lesions.
- Choline levels can be used for the differential diagnosis.
- The probability of malignancy was 17 times higher in patients with choline level >1.65.

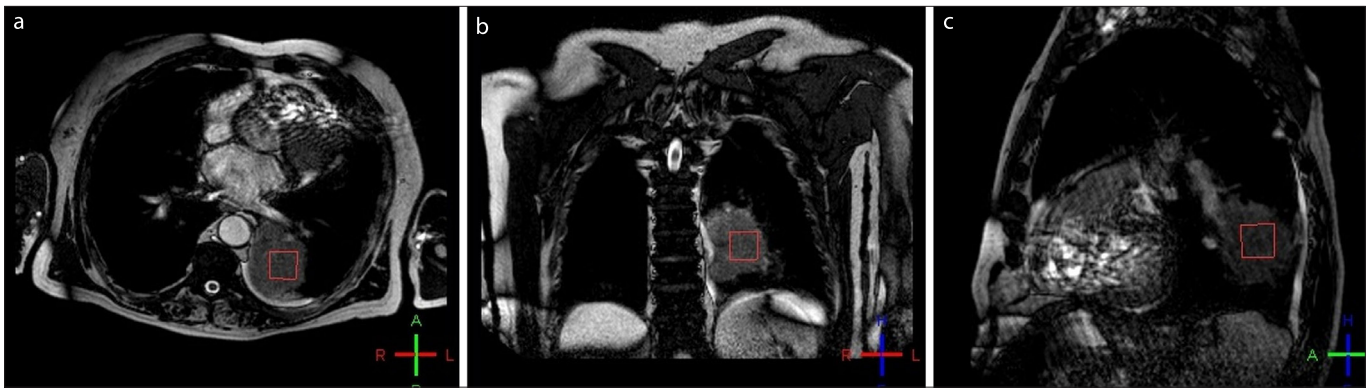

Figure 1.a–c. An 83-year-old male patient diagnosed with squamous cell carcinoma. Axial **(a)**, coronal **(b)**, and sagittal **(c)** views of the lesion are shown. Voxel was placed in the center of the lesion.

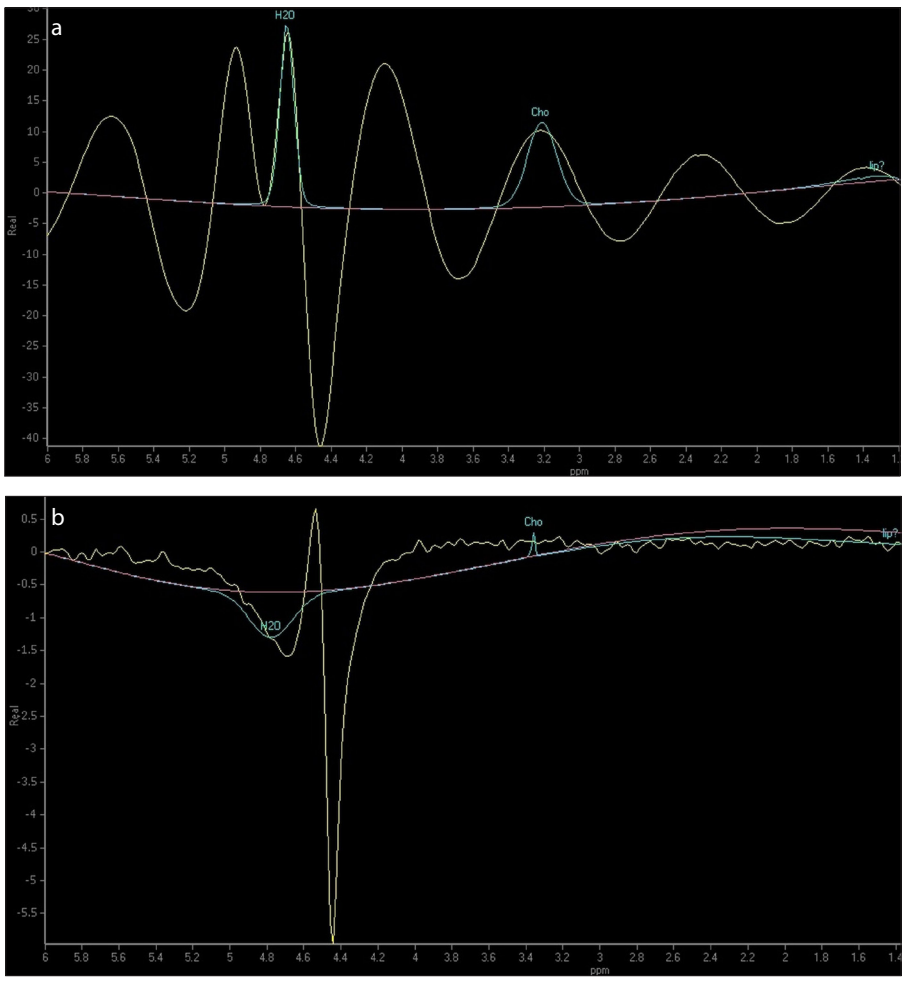

Figure 2. a, b. MRS image **(a)** shows a high choline peak (12) in pulmonary adenocarcinoma. MRS image **(b)** shows a low choline peak (0.3) in a nodule secondary to inflammation.

Ancillary studies like histochemistry and immunohistochemistry were done whenever necessary.

Statistical analysis

Data analysis was performed by using IBM SPSS Statistics version 17.0 software (IBM Corp.). Assumption of normality for continuous variables were examined using Shapiro–Wilk test. Levene test was used for the evaluation of homogeneity of variances. Continuous variables were shown as mean±SD or median (25^{th}–75^{th}) percentiles, where appropriate. Number of cases and percentages were used for categorical data. The mean differences between groups were compared using Student t test. Mann–Whitney U test was applied for the variables which far from normal distribution. Categorical data were analyzed by continuity corrected chi-square or Fisher–Freeman–Halton exact test, where applicable. The optimal cutoff points of each clinical measurement to determine malignancy was evaluated by ROC analyses as giving the maximum sum of sensitivity and specificity for the significant test. Diagnostic performance indicators such as sensitivity, specificity, positive and negative predictive values were also calculated. Multiple logistic regression analysis was performed in order to see the affect of clinical measurements on malignancy after adjustment for all possible confounding factors (i.e., age, gender, maximum nodule size, pack-years cigarette smoking). The Hosmer–Lemeshow test results (χ^2=8.941, df=8 and p = 0.35) indicated that goodness of fit was satisfactory. In addition, Cox & Snell R^2 and Nagelkerke R^2 values were found as 0.37 and 0.49, respectively. Odds ratios and 95% confidence intervals for each independent variable were also calculated. A p value less than 0.05 was considered statistically significant.

Results

According to the pathology results, there was no statistically significant difference between the benign and malignant groups regarding the mean age and gender distribution (p = 0.070 and p = 0.72 respectively) (Table 1).

The benign lung lesions were localized in the right lung in 15 patients (60%) and in the left lung in 10 patients (40%). The malignant lung lesions were localized in the right side in 18 patients (52.9%) and in the

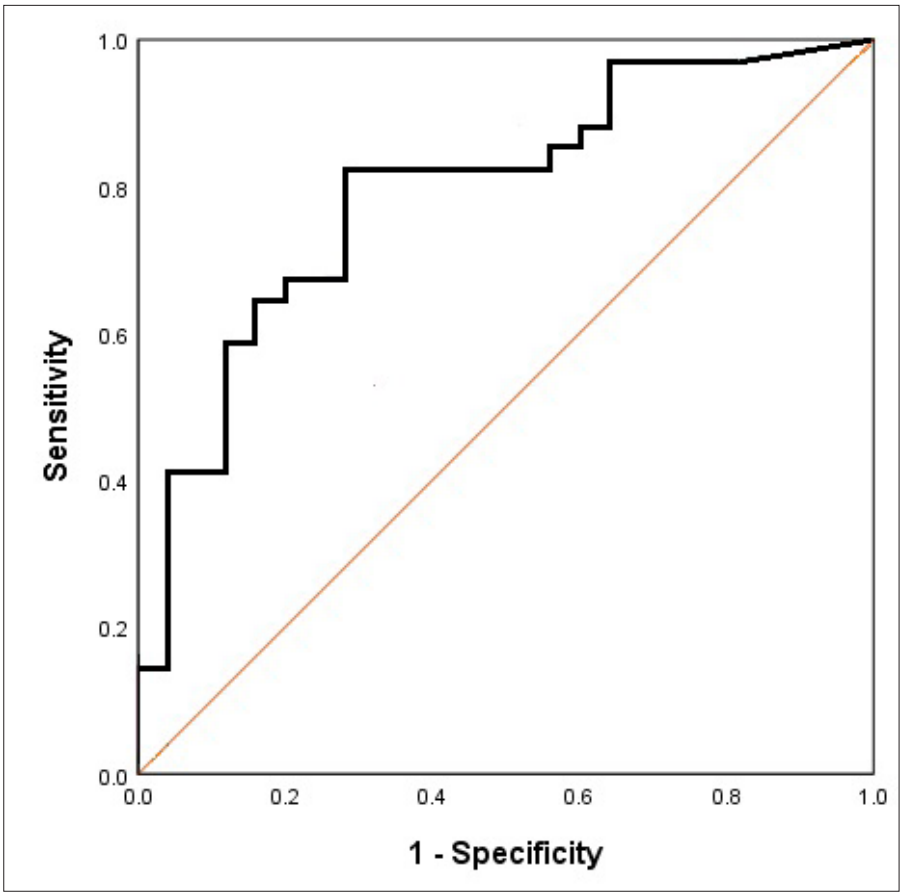

Figure 3. ROC curve for measurements of choline peak correlation with histopathologic groups. AUC: 0.795, 95% CI 0.679–0.911, $p < 0.001$.

Table 2. The indicators of diagnostic performance for discrimination of benign and malignant cases

	Cutoff point	Sensitivity	Specificity	PPV	NPV	Accuracy
Choline	>1.65 µmol/g	82.4%	72.0%	80.0%	75.0%	78.0%

PPV, positive predictive value; NPV, negative predictive value.

Table 3. The results of multiple logistic regression analyses

	OR	95% CI	*p*
Age	1.05	0.98–1.13	0.15
Female factor	1.57	0.28–8.81	0.61
Maximum lesion size	0.99	0.96–1.02	0.61
Pack-years cigarette smoking	1.03	1.00–1.06	0.049
Choline >1.65 µmol/g	17.38	3.78–79.93	<0.001

Multiple logistic regression analyses were conducted after adjustment for all possible confounding factors (i.e., age, gender, maximum lesion size, pack-years cigarette smoking).
OR, odds ratio; CI, confidence interval.

left side in 16 patients (47.1%). Eight (32%) of the benign lesions were localized in the upper lobe, 3 (12%) in the middle segment (middle lobe of the right lung or lingular segment of the left lung) and, 14 (56%) in the lower lobe. Eighteen (52.9%) of the malignant lesions were localized in the upper lobe, 4 (11.8%) in the middle segment (right lung middle lobe or lingular segment of the left lung) and, 12 (35.3%) in the lower lobe. There was no statistically significant difference between the groups regarding the localization (right/left) of the lesions ($p = 0.78$). There was also no statistically significant difference between the groups considering the localization in the lung ($p = 0.23$).

We could also not detect any statistically significant difference between the benign and malignant groups regarding the maximum nodule size ($p = 0.083$). However, the minimum nodule size was significantly larger in the benign group than in the malignant group ($p = 0.023$). In addition, the median smoking (package/year) was significantly higher in the malignant group compared with the benign group ($p = 0.042$) (Table 1).

Eighteen of the patients in the malignant group (52.9%) were diagnosed with adenocarcinoma, 7 (20.6%) with squamous cell carcinoma, 5 (14.7%) with small-cell carcinoma, 3 (8.8%) with metastatic tumors (1 colon and 2 renal cell carcinomas) and 1 patient (3%) with mesothelioma. According to the pathology results, a total of 25 patients were in the benign group: 3 of them were neoplastic; 1 with solitary fibrous tumor (4%), 1 with neurofibroma (4%), and 1 with hamartoma (4%). By histopathological evaluation in the remaining 22 patients, no sign of neoplasm detected. Nineteen patients showed varying amounts of acute or chronic inflammation (76%), 2 with necrotizing granulomatous inflammation (8%), and 1 with round atelectasis (4%).

The choline levels were significantly higher in the malignant group compared with the benign group ($p < 0.001$). Furthermore, the areas under the ROC were also statistically significant between the groups ($p < 0.001$) (Table 1) (Fig. 3).

The most suitable cutoff points of all statistically significant predictive variables, which can be used in the distinguishing of the benign and malignant lesions were listed in Table 2. Cutoff values were calculated for all variables, which had lower and upper limits greater than 0.50 regarding the area under ROC and 95% confidence interval. In addition, diagnostic performance measures such as the sensitivity, specificity, positive and negative predictive value related to the variables were calculated at the best cutoff points and listed in Table 2. We observed that all clinical variables, to which cutoff values were assigned according to other possible confounding factors (e.g., age, gender, nodule size, smoking history), were independent risk factors. After adjusting for age, gender, nodule size, and smoking history, choline remained as an independent indicator for

malignancy. With other factors held constant, the probability of malignancy was 17.38 times higher (95% CI, 3.78–79.93) in patients with a choline >1.65 μmol/g compared with patients with a choline level ≤1.65 μmol/g ($p < 0.001$). All abovementioned evaluations were performed for each significant clinical variable to which a cutoff value was assigned (Table 3).

Discussion

Since pulmonary spectroscopy has not been performed until now, pulmonary MRS application is not available. In this study, breast spectroscopy application was used and choline peak values obtained by supressing water and lipid were calculated. The lack of MRS use for pulmonary lesions is probably due to the mobility of the lungs. We thought that this could be an important challenge for our study. However, it was sufficient for the patients to hold their breath for a short time to obtain the raw images of the spectroscopy. Percutaneous biopsies were performed after MRS because we thought that possible hemorrhage after biopsy might affect the results of the study. In addition, factors such as age, sex, nodule diameter, and smoking, which may also affect the results of the study, were investigated.

During the routine clinical practice, pulmonary nodules or mass lesions may be incidentally detected during chest x-ray or CT examinations (19). Although these lesions may have a malignant character, they may also be benign lesions like cicatrized granuloma, tuberculosis, hamartoma, or arteriovenous malformation (6). The definitive diagnosis of the solitary pulmonary lesions is always difficult. One of the most important goals of diagnostic radiology is to distinguish the benign and malignant lesions with the help of certain noninvasive imaging methods like CT, MRI, or fluorodeoxyglucose positron emission tomography (FDG-PET).

In routine practice, CT is the most common imaging technique used for the detection and diagnosis of pulmonary lesions (20, 21). On CT, the pulmonary nodules cause a prominent density difference due to the air at the background and this prominent contrast difference enables easy identification of the lesions. However, it has limitations in distinguishing benign lesions from malignant ones (22, 23).

In patients with a mass lesion in the lungs, biopsy is a reliable and effective method for definitive diagnosis (7). The lung biopsies can be performed as percutaneous, bronchoscopic and open interventions. Among them, the percutaneous fine-needle biopsy is the most noninvasive technique with specificity and accuracy over 90%, false positivity below 1% and false negativity below 10% (8). However, even relatively noninvasive percutaneous lung biopsies have high complication rates. The risk of pneumothorax is 20.5% and 3.1% of them require thoracic drainage. The reported rates of hemoptysis and mortality were 5.3% and 0.15%, respectively (8). Mortality depends usually on acute massive hemoptysis or pulmonary hemorrhage, pulmonary venous air embolism and severe hemothorax. In the initial studies focused on needle biopsy, the reported risk of the tumor cell seeding along the needle tract was rather low (0.005%) (24). However, later studies showed prominent tumor cell seeding along the needle tract depending on the biological activity of the tumor. Tumor cell seeding rates along the needle tract up to 50% were reported in patients with malignant mesothelioma (25, 26). Furthermore, biopsy is contraindicated in respiratory dysfunctions, respiratory failure, pulmonary hypertension and coagulation anomalies (8). Studies to find noninvasive methods for the differential diagnosis of lung lesions are on-going due to these serious complications and contraindications.

FDG-PET is a noninvasive method that enables the definitive diagnosis of malignant nodules with an accuracy of about 90% (27). However, the sensitivity of FDG-PET declines significantly in lesions with a diameter smaller than 2 centimeters (28). In addition, PET may lead to false positive results in active infections, inflammatory lesions and tuberculoma (29, 30).

Dynamic MRI is used for evaluation of the vascular structure of tumors (microvessel density) and interstitium (ratio of elastic and collagen fibers) and for prediction of prognosis in patients with peripheral-type small cell lung cancer (31). Studies demonstrated that kinetic indexes and morphological parameters of MRI enable accurate differentiation of malignant and benign lesions (32–34). However, as with PET, it is difficult to distinguish acute inflammatory lesions from active infections and malignant lesions also on MRI (35).

Early diagnosis is a critical factor in cancer treatment. Conventional imaging methods display the presence of the lesion and its morphology, while spectroscopy evaluates the chemical composition of the cells. Therefore, evaluations done with the combination of MRI and MRS provides important information regarding the early diagnosis of cancers in different organs and tissues, particularly in neurological tissues (36). MRS is an analytic method used in chemistry for the evaluation of the molecules and their biophysical properties. The MRI spectrums may be obtained from various metabolites in the human body using several nuclei like ^{1}H, ^{31}P, ^{19}F, ^{13}C, and ^{23}Na. However, as ^{1}H nucleus has a high sensitivity and is abundantly found in many metabolites, it is widely used in MRS (37).

It is well known that cancer cells have an abnormal choline and lipid metabolism (38). Therefore, in our study, we evaluated choline levels in pulmonary lesions with MRS. Compounds that contain high levels of cellular phosphocholine and total choline are observed in cancer cells and tumor tissue and are related to malignant transformation, invasion, and metastasis (39, 40). Increase in compounds containing high levels of cellular phosphocholine and total choline is one of the most common features of cancers like ovarian, prostate, lung, and bladder cancers (40–45).

MRS results revealed that there was a stastistically significant difference between the benign and malignant groups regarding choline levels. The high levels of choline indicate that it may be used for the differential diagnosis of pulmonary lesions similar to the malignant lesions in other organs. In a case report published on this subject, it was also stated that the choline peak can be used to detect lung cancer, in support of our study (17).

We also calculated the cutoff values of the statistically significant parameters and we determined that these parameters were independent of all other confounding factors. For example, after adjusting for age, gender, nodule size, and smoking, choline remained as an independent indicator of malignancy. If other factors held constant, the probability of the malignancy was 17.38 times higher (95% CI, 3.78–79.93) in patients with a choline level above 1.65 μmol/g compared to the patients with a choline level lower than 1.65 μmol/g ($p < 0.001$). Sensitivity and specificity were calculated as 82.4% and 72%, respectively, for choline values with ROC analysis.

The small subject size was one of the limitations of our study. Besides this, only choline levels were measured. In future prospective studies, a broader spectrum of metabolites can be investigated. Furthermore, researches may also focus on lung-specific metabolites.

In conclusion, MRS, is a noninvasive method that can be used in the differential diagnosis of pulmonary nodules and mass lesions. Our study is the first trial focused on this topic. Future studies encouraged by these findings may facilitate the routine use of MRS in the differential diagnosis of lung lesions instead of biopsy, similar to its use in the brain and other organs.

Conflict of interest disclosure

The authors declared no conflicts of interest.

References

1. Midthun DE, Swensen SJ, Jett JR. Approach to the solitary pulmonary nodule. Mayo Clin Proc 1993; 68:378–385. [Crossref]
2. Lillington GA. Management of solitary pulmonary nodules: how to decide when resection is required. Postgrad Med 1997; 101:145–150. [Crossref]
3. Brandman S, Ko JP. Pulmonary nodule detection, characterization, and management with multidetector computed tomography. J Thorac Imaging 2011; 26:90–105. [Crossref]
4. Albert RH, Russell JJ. Evaluation of the solitary pulmonary nodule. Am Fam Physician 2009; 80:827–831.
5. Pasławski M, Krzyzanowski K, Złomaniec J, Gwizdak J. Morphological characteristics of malignant solitary pulmonary nodules. Ann Univ Mariae Curie Sklodowska Med. 2004; 59:6–13.
6. Murrmann GB, van Vollenhoven FH, Moodley L. Approach to a solid solitary pulmonary nodule in two different settings-"Common is common, rare is rare". J Thorac Dis 2014; 6:237–248.
7. Lorenz J, Blum M. Complications of percutaneous chest biopsy. Semin Intervent Radiol 2006; 23:188–193. [Crossref]
8. Manhire A, Charig M, Clelland C, et al. Guidelines for radiologically guided lung biopsy. Thorax 2003; 58:920–936. [Crossref]
9. Noguerol TM, González JS, Barbero JPM, Figueiras RG, González BG, Luna A. Clinical imaging of tumor metabolism with 1H magnetic resonance spectroscopy. Magn Reson Imaging Clin N Am 2016; 24:57–86. [Crossref]
10. Salibi N, Brown MA. Clinical MR spectroscopy. New York, NY: Wiley-Liss, 1998; 20–22.
11. Lean C, Doran S, Somorjai RL, et al. Determination of grade and receptor sta¬tus from the primary breast lesion by magnetic resonance spectroscopy. Technol Cancer Res Treat 2004; 3:551–556. [Crossref]
12. Khan SA, Cox IJ, Hamilton G, Thomas HC, Taylor-Robinson SD. In vivo and in vitro nuclear future directions of NMR magnetic resonance spectroscopy as a tool for investigating hepatobiliary disease: a review of 1H and 31P MRS applications. Liver Int 2005; 25:273–281. [Crossref]
13. Cho SG, Lee DH, Lee KY, et al. Differentiation of chronic focal pancreatitis from pancreatic carcinoma by in vivo proton magnetic resonance spectroscopy. J Comput Assist Tomogr 2005; 29:163–169. [Crossref]
14. Verma S, Rajesh A, Fütterer JJ, et al. Prostate MRI and 3D MR Spectroscopy: How We Do It. AJR Am J Roentgenol 2010; 194:1414–1426. [Crossref]
15. Chen W, Zu Y, Huang Q, et al. Study on metabonomic characteristics of human lung cancer using high resolution magic-angle spinning 1H NMR spectroscopy and multivariate data analysis. Magn Reson Med 2011; 66:1531–1540. [Crossref]
16. Hanaoka H, Yoshioka Y, Ito I, Niitu K, Yasuda N. In vitro characterization of lung cancers by the use of 1H nuclear magnetic resonance spectroscopy of tissue extracts and discriminant factor analysis. Magn Reson Med 1993; 29:436–440. [Crossref]
17. Fujimoto S, Minato K, Horikoshi H, et al. Proton magnetic resonance spectroscopy of lung cancer in vivo. Radiol Case Rep 2020; 15:1099–1102. [Crossref]
18. Kim M. Cecil. Proton magnetic resonance spectroscopy: technique for the neuroradiologist. Neuroimaging Clin N Am 2013; 23:381–392. [Crossref]
19. Edey AJ, Hansell DM. Incidentally detected small pulmonary nodules on CT. Clin Radiol 2009; 64:872–884. [Crossref]
20. Brenner DJ, Hall EJ. Computed tomography—an increasing source of radiation exposure. N Engl J Med 2007; 357:2277–2284. [Crossref]
21. Fass L. Imaging and cancer: a review. Mol Oncol 2008; 2:115–152. [Crossref]
22. Bach PB, Mirkin JN, Oliver TK, et al. Benefits and harms of CT screening for lung cancer: a systematic review. JAMA 2012; 307:2418–2429. [Crossref]
23. Kim H, Park CM, Goo JM, Wildberger JE, Kauczor HU. Quantitative computed tomography imaging biomarkers in the diagnosis and management of lung cancer. Invest Radiol 2015; 50:571–583. [Crossref]
24. Charboneau JW, Reading CC, Welch TJ. CT and sonographically guided needle biopsy: current techniques and new innovations. AJR Am J Roentgenol 1990; 154:1–10. [Crossref]
25. Agarwal PP, Seely JM, Matzinger FR, et al. Pleural mesothelioma: sensitivity and incidence of needle track seeding after image-guided biopsy versus surgical biopsy. Radiology 2006; 241:589–594. [Crossref]
26. Metintas M, Ozdemir N, Isiksoy S, et al. CT-guided pleural needle biopsy in the diagnosis of malignant mesothelioma. J Comput Assist Tomogr 1995; 19:370–374. [Crossref]
27. Kostakoglu L, Agress H Jr, Goldsmith SJ. Clinical role of FDG PET in evaluation of cancer patients. RadioGraphics 2003; 23:315–340. [Crossref]
28. Mastin ST, Drane WE, Harman EM, Fenton JJ, Quesenberry L. FDG SPECT in patients with lung masses. Chest 1999; 115:1012–1017. [Crossref]
29. Goldsmith SJ, Kostakoglu L. Nuclear medicine imaging of lung cancer. Radiol Clin North Am 2000; 38:511–524. [Crossref]
30. Goo JM, Im JG, Do KH, et al. Pulmonary tuberculoma evaluated by means of FDG PET: findings in 10 cases. Radiology 2000; 216:117–121. [Crossref]
31. Fujimoto K, Abe T, Müller NL, et al. Small peripheral pulmonary carcinoma evaluated with dynamic MR imaging: correlation with tumor vascularity and prognosis. Radiology 2003; 227:786–793. [Crossref]
32. Schaefer JF, Vollmar J, Schick F, et al. Solitary pulmonary nodules: dynamic contrast-enhanced MR imaging: perfusion differences in malignant and benign lesions. Radiology 2004; 232:544–553. [Crossref]
33. Ohno Y, Hatabu H, Takenaka D, Adachi S, Kono M, Sugimura K. Solitary pulmonary nodules: Potential role of dynamic MR imaging in management: initial experience. Radiology 2002; 224:503–511. [Crossref]
34. Kono R, Fujimoto K, Terasaki H, et al. Dynamic MRI of solitary pulmonary nodules: comparison of enhancement patterns of malignant and benign small peripheral lung lesions. AJR Am J Roentgenol 2007; 188:26–36. [Crossref]
35. Fujimoto K. Usefulness of contrast-enhanced magnetic resonance imaging for evaluating solitary pulmonary nodules. Cancer Imaging 2008; 8:36–44.[Crossref]
36. Bezabeh T, Ijare OB, Nikulin AE, Somorjai RL, Smith IC. MRS-based Metabolomics in Cancer Research. Magn Reson Insights 2014; 7:1–14.
37. van der Graf M. In vivo magnetic resonance spectroscopy: basic methodology and clinical applications. Eur Biophys J 2010; 39:527–540. [Crossref]
38. Mori N, Wildes F, Takagi T, Glunde K, Bhujwalla ZM. The tumor microenvironment modulates choline and lipid metabolism. Front Oncol 2016; 6:262. [Crossref]
39. Glunde K, Bhujwalla ZM, Ronen SM. Choline metabolism in malignant transformation. Nat Rev Cancer 2011; 11:835–848. [Crossref]
40. Aboagye EO, Bhujwalla ZM. Malignant transformation alters membrane choline phospholipid metabolism of human mammary epithelial cells. Cancer Res 1999; 59:80–84.
41. Ramirez de Molina A, Gutierrez R, Ramos MA, et al. Increased choline kinase activity in human breast carcinomas: clinical evidence for a potential novel antitumor strategy. Oncogene 2002; 21:4317–4322. [Crossref]
42. Iorio E, Ricci A, Bagnoli M, et al. Activation of phosphatidylcholine cycle enzymes in human epithelial ovarian cancer cells. Cancer Res 2010; 70:2126–2135. [Crossref]
43. Ackerstaff E, Pflug BR, Nelson JB, Bhujwalla ZM. Detection of increased choline compounds with proton nuclear magnetic resonance spectroscopy subsequent to malignant transformation of human prostatic epithelial cells. Cancer Res 2001; 61:3599–3603.
44. Ramirez de Molina A, Sarmentero-Estrada J, Belda-Iniesta C, et al. Expression of choline kinase alpha to predict outcome in patients with early-stage non-small-cell lung cancer: a retrospective study. Lancet Oncol 2007; 8:889–897. [Crossref]
45. Hernando E, Sarmentero-Estrada J, Koppie T, et al. A critical role for choline kinase-alpha in the aggressiveness of bladder carcinomas. Oncogene 2009; 28:2425–2435. [Crossref]